

Synthesis and Characterization of Core–Shell GaP@GaN and GaN@GaP Nanowires

Hung-Min Lin,[†] Yong-Lin Chen,[‡] Jian Yang,[†] Yao-Chung Liu,[†] Kai-Min Yin,[§] Ji-Jung Kai,[§] Fu-Rong Chen,[§] Li-Chyong Chen,^{‡,||} Yang-Fang Chen,[‡] and Chia-Chun Chen^{*,†,⊥}

Department of Chemistry, National Taiwan Normal University, 88 Sec. 4 Tingchow Road, Taipei 116, Taiwan, Department of Engineering and System Science, National Tsinghua University, Hsin-Chu, Taiwan, Department of Physics and Center for Condensed Matter Science, National Taiwan University, Taipei, Taiwan, and Institute of Atomic and Molecular Sciences, Academia Sinica, Taipei, Taiwan

Received January 8, 2003; Revised Manuscript Received February 12, 2003

ABSTRACT

A convenient thermal CVD route to core–shell GaP@GaN and GaN@GaP nanowires is developed. The structural analyses indicate that the nanowires exhibit a two-layer and wirelike structure. High-resolution transmission electron microscopy (HRTEM) images reveal misfit dislocation loops at the interface of the nanowires. Unusual temperature dependences of the photoluminescence (PL) intensity of GaP@GaN nanowires are observed, and they are interpreted by the piezoelectric effect induced from lattice mismatch between two semiconductor layers. In the Raman spectra of GaN@GaP nanowires, an unexpected peak at 386 cm⁻¹ is found and assigned to a surface phonon mode.

Semiconductor heterostructures play an important role in modern device physics because of great contributions to fundamental research and practical optoelectronic devices.¹ The structures have been constructed in many current electronic devices on the basis of their unique optical, electronic, and structural characteristics generated from the interfaces of two semiconductors. Numerous studies have been reported on the heterostructures of a multilayer thin film (quantum well), a typical 2-D nanostructure.² Also, the studies of heterostructures of 0-D nanostructure (semiconductor quantum dots (nanocrystals)) have demonstrated several unusual optical and structural properties. For instance, the fluorescence of core–shell quantum dots has been strongly enhanced mainly because of a large band-gap difference between core and shell semiconductors.³ Preparations of heterostructures of semiconductor nanowires (1-D nanostructures) have also been developed recently. For example, single-crystalline Si/SiGe superlattice nanowires were synthesized by a hybrid pulsed laser ablation and chemical vapor deposition process.⁴ Nanowhiskers composed of InP and InAs segments were grown by rapidly switching

between different sources.⁵ Core–shell, multishell, or multilayer Si–Ge nanowires were synthesized by a two-step chemical vapor deposition route.⁶ The route mainly consists of axial growth based on a vapor–liquid–solid (VLS) mechanism and shell growth based on homogeneous vapor deposition. GaN nanorods encapsulated by carbon nanotubes (GaN@CNT) were synthesized by the deposition of carbon from the thermolysis of methane on the surface of GaN nanorods.⁷ Helical crystalline silicon carbide nanowires covered with a silicon oxide sheath (SiC@SiO₂) have been synthesized by a chemical vapor deposition technique.⁸

The studies of III–V semiconductor nanowires and nanorods have shown a great potential in the fabrications of prototype optoelectronic devices such as nanowire lasers, sensors, and transistors.⁹ However, to our knowledge, there are still very few reports on core–shell nanowires of III–V semiconductors, although single-component nanowires such as GaN and GaP nanowires have been successfully prepared via various vapor deposition techniques.^{10–13} For example, GaN and GaP nanowires were synthesized by laser ablation on targets, which were composed of elements desired in nanowires and catalysts.¹⁰ Later, laser ablation on a mixture of GaN (or GaP) and Ga₂O₃ was also used to prepare crystalline GaN (or GaP) nanowires coated with an amorphous Ga₂O₃ layer.¹¹ In addition, a convenient thermal CVD route to high-quality GaN nanowires has been reported.¹²

* To whom correspondence should be addressed. E-mail: t42005@cc.ntnu.edu.tw.

[†] National Taiwan Normal University.

[‡] Department of Physics, National Taiwan University.

[§] National Tsinghua University.

^{||} Center for Condensed Matter Science, National Taiwan University.

[⊥] Academia Sinica.

Recently, GaP nanowires have been achieved by the thermal deposition of Ga(P'Bu₂) in the presence of surfactants or the sublimation of ball-milled powders at 1100 °C.¹³

In this report, typical direct and indirect band-gap III–V semiconductors, GaN and GaP, are chosen for the construction of core–shell nanowires. We would expect that the different band-gap characteristics at the interface between GaN and GaP layers of core–shell nanowires should offer many opportunities for us to study their unique optical and structural properties. Here, we have developed a two-step synthetic technique and have successfully prepared core–shell GaP@GaN and GaN@GaP nanowires. The core–shell nanowire structures were characterized using scanning electron microscopy (SEM), TEM, PL, and Raman spectroscopy. The PL spectra of GaP@GaN nanowires revealed an interesting temperature-dependence behavior, and an unexpected surface phonon signal was observed in the Raman spectra of GaN@GaP nanowires.

Preparation of GaP@GaN Nanowires. GaP nanowires were grown on a silicon wafer from the reaction of molten gallium, red phosphor, and iron phthalocyanine at 1000 °C for 30 min. The wafer with GaP nanowires facing down was placed on the top of a boat containing gallium and gallium oxide. The boat was inserted into a tube furnace and then heated at 950 °C for 3 h under a flow of ammonia gas (10 sccm). Finally, the resulting sample was collected from the wafer for the characterization.

Preparation of GaN@GaP Nanowires. GaN nanowires were grown on a silicon wafer by the reaction of gallium and ammonia gas at 950 °C in the presence of metal phthalocyanine according to our previous reports.¹² As in the description above, the wafer was placed on a boat containing gallium, gallium oxide, and red phosphor. The boat was then heated at 1000 °C for 30 min under argon (5 sccm) to obtain the final products on the wafer. Careful control of the reaction temperature and time is necessary for the successful preparation of both core–shell nanowires.

A typical X-ray diffraction (XRD) pattern of the obtained GaP@GaN nanowires is shown in Figure 1a. The diffraction peaks can be indexed as a zinc blende phase GaP (JCPDS Card, 32-397) and a wurtzite phase GaN (JCPDS Card, 2-1078). The lattice constants calculated from the pattern are $a = 5.44$ Å for GaP and $a = 3.18$ Å, $c = 5.17$ Å for GaN, which are in excellent agreement with the reported values.^{12,13} Only the diffraction peaks of GaP and GaN and no characteristic peaks of elemental gallium or gallium oxide are observed in the pattern. Figure 1b shows the XRD pattern of GaN@GaP nanowires. The positions of the diffraction peaks are the same as those in Figure 1a, and the change on the relative peak intensity of GaP and GaN are found. These results confirm that GaP and GaN phases coexisted in the samples.

A typical SEM image of GaP@GaN core–shell nanowires is shown in Figure 2a. Numerous wirelike structures with smooth surfaces and a uniform diameter were observed in the images. The diameters of core–shell nanowires were in the range of 20–150 nm, and their lengths were up to several micrometers. Similar results were also observed in the SEM

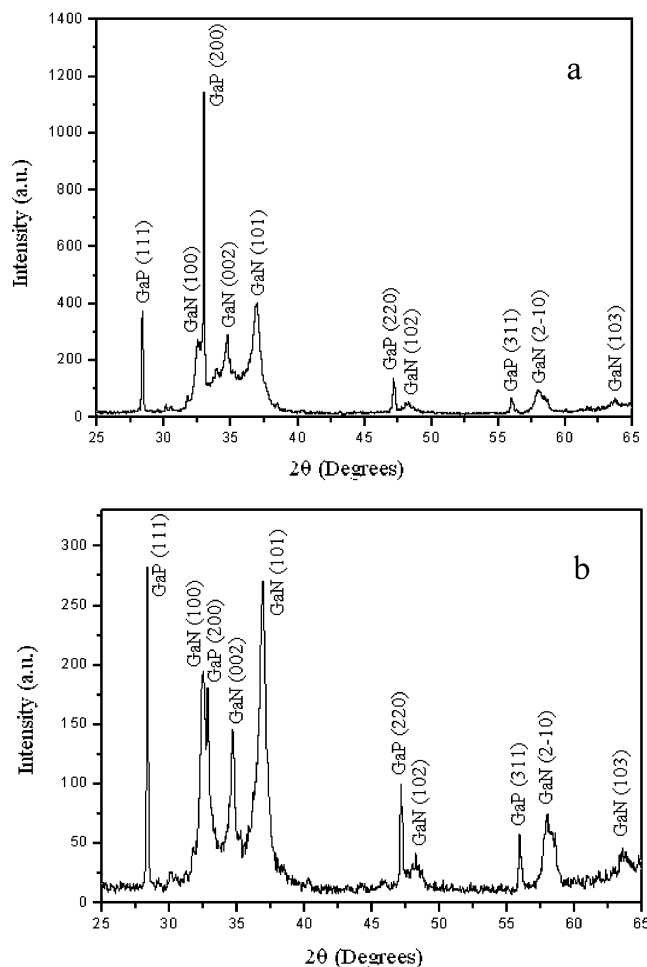


Figure 1. XRD patterns and diffraction indexes of (a) core–shell GaP@GaN nanowires and (b) core–shell GaN@GaP nanowires.

images of GaN@GaP core–shell samples. The HRTEM images of a single GaN@GaP nanowire and a single core–shell GaP@GaN nanowire are presented in Figure 2b and c, respectively. The great contrast difference between the center and the edge of the nanowires in both images indicates that the nanowires indeed have a two-layer structure. Typically, the thickness of the shell layer was in the range of 4–20 nm, and the diameter of the core in the nanowires was in the range of 10–100 nm, depending on reaction conditions. Energy-dispersive X-ray spectroscopy (EDX) of these two-layer structures was used to determine the elemental composition of the nanowires qualitatively. The results suggested that the outer layer in Figure 2c was composed of only a single component (GaP or GaN) and that the inner layer was composed of both GaN and GaP. Figure 2d shows an enlarged image of a single GaP@GaN nanowire. The image exhibits clear lattice fringes and crystal facets at the lateral surface of the nanowire. The lattice image can be assigned to a core–shell structure of GaP nanowires encapsulated inside GaN crystals. Moreover, although Figure 2c is a projected view of a GaP@GaN nanowire, the interface of GaP@GaN can be easily identified from the termination of defects running across the nanowire. These defects are thought to be misfit dislocation loops (indicated by the arrow

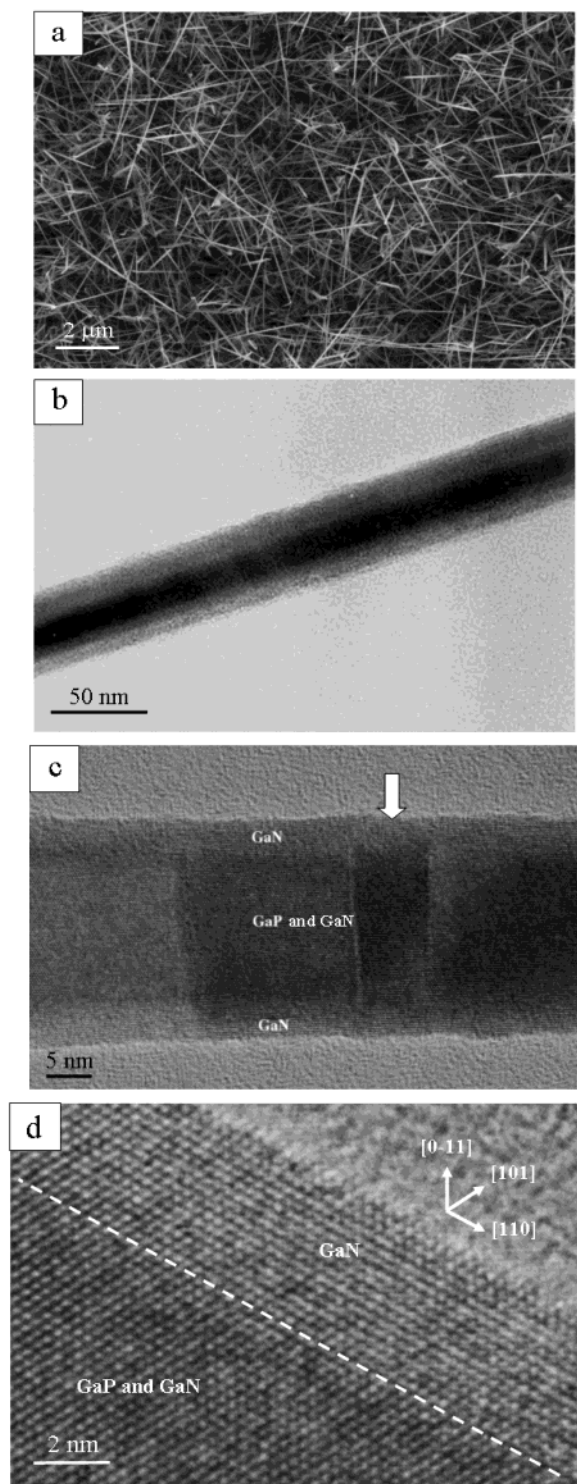


Figure 2. (a) SEM image of GaP@GaN core-shell nanowires. (b) HRTEM image of a single core-shell GaN@GaP nanowire to show a two-layer structure clearly. (c) HRTEM image of a single core-shell GaP@GaN nanowire. Clear lattice fringes are observed in the image. The misfit dislocation loop is found in the image and is indicated by an arrow. The elemental compositions of the inner and outer layers were characterized qualitatively using EDX and are indicated in the image. The beam size of HRTEM is about 0.5 nm. (d) Enlarged HRTEM image of a single core-shell GaP@GaN nanowire. The interface between two semiconductor layers is highlighted by a dashed line. The growth direction of the GaN shell is indicated. The [110] direction is commonly observed in GaN nanowires.

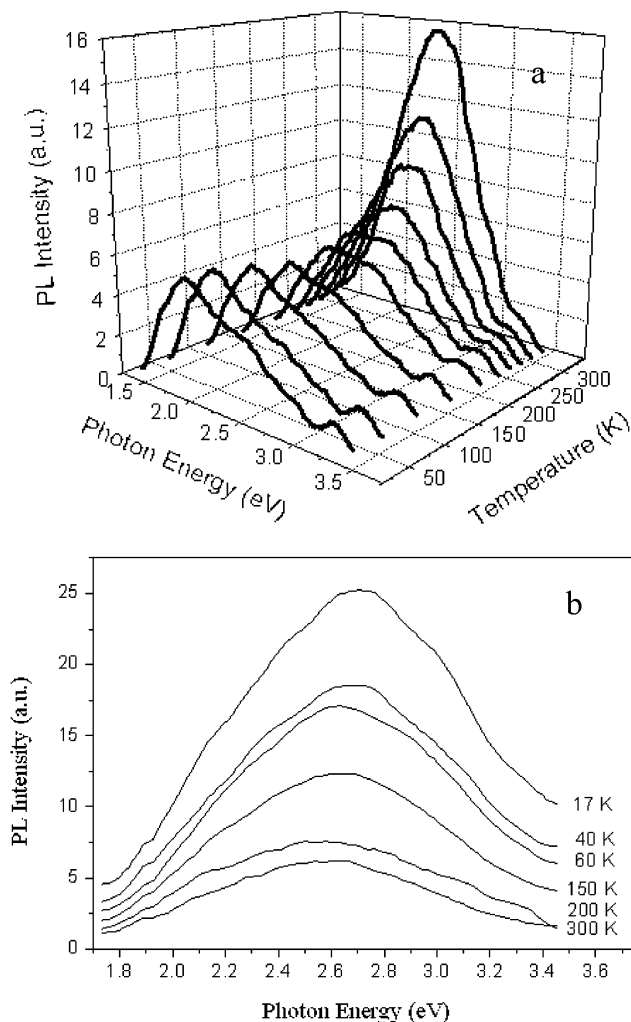


Figure 3. Photoluminescence spectra of (a) core-shell GaP@GaN nanowires and (b) core-shell GaN@GaP nanowires at various temperatures.

in Figure 2c) around the nanowire to accommodate the lattice misfit between GaP and GaN.

The SEM and TEM results have suggested that core-shell nanowires were observed in our resulting samples, but no junctionlike nanowires or single-component nanowires were found. Thus, the whole reaction mechanism can be understood as the following: the core nanowires (GaP/GaN) were first formed through a VLS mechanism.^{6,10} Then, the core nanowires served as nuclei, and the semiconductor on the shell (GaN/GaP) was directly deposited onto the core through a VS mechanism. Therefore, the shell structures were formed mainly through radial but not axial growth.

Figure 3a presents the PL spectra of core-shell GaP@GaN nanowires at different temperatures. The same point of those spectra is a broad PL peak from 1.5 to 3.5 eV in every spectrum. The main peak position is 2.46 eV at room temperature. Since the reported PL signal of GaP nanowires is located around 2.28 to 2.40 eV and the contribution of strain from the GaN layer should be taken into account, it is reasonable to assume that the peak at 2.46 eV arises from the encapsulated GaP nanowires. Those spectral data are confirmed by strain analysis based on a biaxial strain model

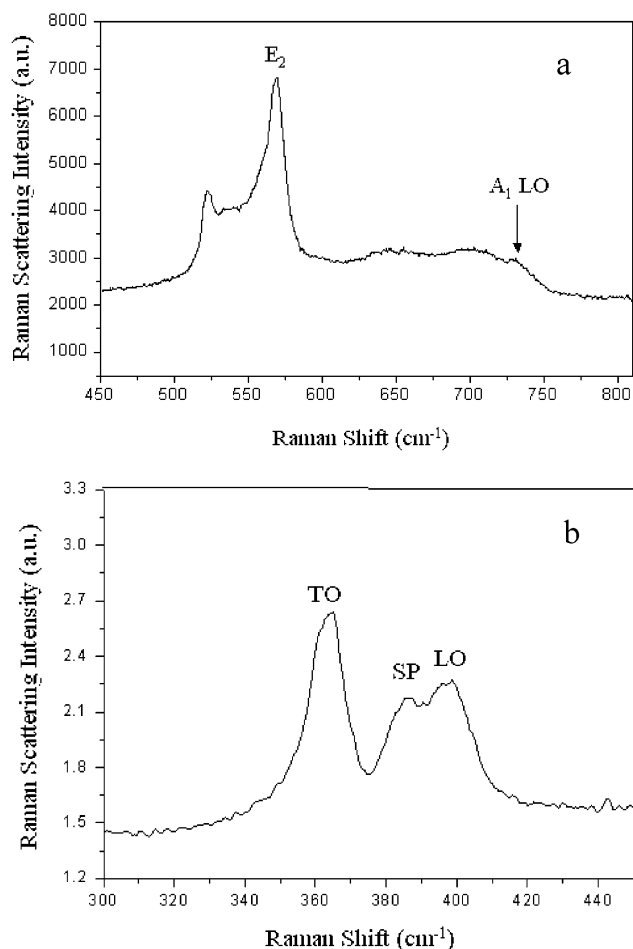


Figure 4. Raman spectra of (a) core-shell GaP@GaN nanowires and (b) core-shell GaN@GaP nanowires at room temperature.

in quantum films. The theoretical strain-induced energy shift is computed to be about 200 meV, which is very close to the observed energy shift (~ 180 meV) between the PL peak of GaN@GaP (2.46 eV) and that of GaP nanowires (2.28 eV) at room temperature. However, further details on those theoretical calculations will be published elsewhere.¹⁴

An interesting temperature dependence in which the intensity of the PL peak at room temperature is much stronger than that at low temperature was observed in the PL spectra of core-shell GaP@GaN nanowires. This surprising result violates the usual thermal quenching behavior. It is believed that it may result from the piezoelectric effect due to the different thermal expansion coefficients of GaN and GaP in these coaxial nanowires. The linear thermal coefficient of GaP is in the range of $(3.5\text{--}4.7) \times 10^{-6} \text{ K}^{-1}$ from 200 to 300 K,¹⁵ which is larger than that of GaN $((2.5\text{--}3.4) \times 10^{-6} \text{ K}^{-1})$.¹⁶ When these core-shell nanowires are cooled from room temperature, the inside GaP core will contract more quickly than the outside GaN sheath. Then the internal strain and the piezoelectric field are gradually relaxed. Therefore, the charges induced by the piezoelectric field are reduced, which leads to a decrease in the radiative recombination probability and emission efficiency. This process results in the abnormal temperature dependence in PL spectra. This phenomenon indirectly confirms the core-shell heterostruc-

tures in nanowires. However, the presence of strain and piezoelectric effects shows that the core-shell heterostructure has a great influence on the electronic and optical properties of nanocrystals.

Although PL peaks of core-shell GaN@GaP nanowires also present a blue shift, the peaks exhibit a normal temperature dependence caused by thermal quenching behavior, as shown in Figure 3b. The reason may be that the linear thermal coefficient of GaP is larger than that of GaN, which will increase the strain on the interface at low temperature, so the piezoelectric effect caused by the strain is increased. As a result, heterostructure nanowires exhibit normal PL behavior.

The Raman spectra of core-shell GaP@GaN nanowires are shown in Figure 4a. The two signals at 569 and 729 cm^{-1} are undoubtedly attributed to the E_2 and $A_1(\text{LO})$ modes of GaN.¹² Another signal at 521 cm^{-1} can be assigned to the silicon wafer.¹⁷ No signals coming from GaP are observed in this spectrum. Since Raman scattering is a surface phenomenon, Raman spectra on core-shell nanowires mainly present Raman scattering peaks of shell materials. This is also confirmed by the Raman spectrum from core-shell GaN@GaP nanowires. However, the Raman spectra of the GaN@GaP nanowires exhibit an unexpected signal at 386 cm^{-1} besides the TO (364 cm^{-1}) and LO (398 cm^{-1}) modes of GaP, as shown in Figure 4b. This signal between the TO and LO modes of GaP is demonstrated to be a surface phonon mode related to the heterostructures by the shape-dependent depolarization factor and the dielectric response-function model, which will be published elsewhere in detail.¹⁴ The appearance of the surface phonon proved the core-shell nanostructure from the side.

In conclusion, core-shell GaP@GaN and GaN@GaP nanowires were successfully synthesized, and their structural and optical properties were investigated. Further studies of the diameter and thickness dependence on their PL and Raman spectra are currently in progress. In addition, studies on their other physical properties such as electron-electron interactions and charge-carrier confinement in the core-shell nanowires will be continued in the future.

Acknowledgment. Financial support of this work from the NSC, NTNU (ORD92-3), and National Science and Technology Program is gratefully acknowledged. We thank Mr. Chih-Jung Hsu for beneficial discussions.

References

- (1) (a) Einspruch, N. G.; Frensley, W. R. *Heterostructures and Quantum Devices*; Academic Press: San Diego, CA, 1994. (b) Ivchenko, E. L.; Pikus, G. E. *Superlattices and Other Heterostructures: Symmetry and Optical Phenomena*; Springer: Berlin, 1997.
- (2) (a) Kittel, C. *Introduction to Solid-State Physics*, 7th ed.; Wiley & Sons: New York, 1996. (b) Peter, S. Z. *Quantum Well Laser*; Academic Press: San Diego, CA, 1993. (c) Araujo, C. P.; Scott, J. F.; Taylor, G. W. *Ferroelectric Thin Films: Synthesis and Basic Properties*; Gordon and Breach Publishers: Amsterdam, 1996.
- (3) (a) Cao, Y. W.; Banin, U. *Angew. Chem., Int. Ed.* **1999**, *38*, 3692. (b) Peng, X.; Schlamp, M. C.; Kadavanich, A. V.; Alivisatos, A. P. *J. Am. Chem. Soc.* **1997**, *119*, 7019. (c) Dabbousi, B. O.; Rodriguez-Viejo, J.; Mikulec, F. V.; Heine, J. R.; Mattoussi, H.; Ober, R.; Jensen, K. F.; Bawendi, M. G. *J. Phys. Chem. B.* **1997**, *101*, 9463.
- (4) Wu, Y.; Fan, R.; Yang, P. *Nano. Lett.* **2002**, *2*, 83.

- (5) (a) Ohlsson, B. J.; Magnusson, M. H.; Bjork, M. T.; Wallenberg, L. R.; Deppert, K.; Samuelson L. *Appl. Phys. Lett.* **2001**, 79, 3335. (b) Bjork, M. T.; Ohlsson, B. J.; Sass, T.; Persson, A. I.; Thelander, C.; Magnusson, M. H.; Deppert, K.; Wallenberg, L. R.; Samuelson, L. *Nano. Lett.* **2002**, 2, 87.
- (6) Lauhon, L. J.; Gudiksen, M. S.; Wang, C. L.; Lieber, C. M. *Nature (London)* **2002**, 420, 57.
- (7) Chen, C.-C.; Yeh, C.-C.; Liang, C.-H.; Lee, C.-C.; Chen, C.-H.; Yu, M.-Y.; Liu, H.-L.; Chen, L.-C.; Lin, Y.-S.; Ma, K.-J.; Chen, K.-H. *J. Phys. Chem. Solids* **2001**, 62, 1577. (b) Han, W.; Zettl, A. *Adv. Mater.* **2002**, 14, 1560.
- (8) Zhang, H. F.; Wang, C. M.; Wang, L. S. *Nano. Lett.* **2002**, 2, 941.
- (9) (a) Johnson, J.; Choi, H. J.; Knutsen, K. P.; Schaller, R. D.; Saykally, R. J.; Yang, P. *Nat. Mater.* **2002**, 1, 101. (b) Cui, Y.; Wei, Q.; Park, H.; Lieber, C. M. *Science (Washington, D.C.)* **2001**, 293, 1289. (c) Duan, X.; Huang, Y.; Cui, Y.; Wang, J.; Lieber, C. M. *Nature (London)* **2001**, 409, 66.
- (10) Duan, X. F.; Lieber, C. M. *Adv. Mater.* **2000**, 12, 298.
- (11) Shi, W.; Zheng, Y.; Wang, N.; Lee, C. S.; Lee, S. T. *Adv. Mater.* **2001**, 13, 591.
- (12) (a) Chen, C.-C.; Yeh, C.-C.; Chen, C.-H.; Yu, M.-Y.; Liu, H.-L.; Wu, J.-J.; Chen, K.-H.; Chen, L.-C.; Peng, J.-Y.; Chen, Y.-F. *J. Am. Chem. Soc.* **2001**, 123, 2791. (b) Chen, C.-C.; Yeh, C.-C. *Adv. Mater.* **2000**, 12, 738.
- (13) (a) Kim, Y. H.; Jun, Y. W.; Jun, B. H.; Lee, S. M.; Cheon, J. *J. Am. Chem. Soc.* **2002**, 124, 13656. (b) Seo, H. W.; Bae, S. Y.; Park, J.; Yang, H.; Kim, S. *Chem. Commun.* **2002**, 2564.
- (14) Chen, Y.-L.; Huang, L.-Y.; Chen, Y.-F.; Yu, M.-Y.; Chen, C.-C. *Phys. Rev. B*, in press.
- (15) Deus, P.; Voland, U.; Schneider, H. A. *Phys. Status Solidi A* **1983**, 80, K29.
- (16) Sheleg, A. U.; Savastenko, V. A.; Vesti, A. *Nauk BSSR, Ser. Fiz. Mater. Nauk* **1976**, 3, 126.
- (17) Wu, J. J.; Wong, T. C.; Yu, C. C. *Adv. Mater.* **2002**, 14, 1643.

NL0340125